Propulsive Performance of Pitching Panels with Bio-Inspired Passive Directional Flexibility

Ruijie Zhu[1], Junshi Wang[2], Gregory Lewis[3], Joseph Zhu[4], Haibo Dong[5], Hilary Bart-Smith[6]
University of Virginia, Charlottesville, VA, 22903

Dylan Wainwright[7], George Lauder[8]
Harvard University, Cambridge, MA 02138

Thunniform swimming—as displayed by tuna and mackerel—is recognized as fast and efficient. For this study, we have retrieved the first set of high-resolution videos of tuna swimming in two orthogonal directions in sync. From observing tuna swimming, the majority of motion happens within posterior one-third of the body, which mainly consists of peduncle with rotational freedom and flexible caudal fin. It has been shown that choosing the optimal flexibility for flapping aerofoil panel or artificial fin can boost the thrust or efficiency by over 100%, due to change in fin kinematics and wake structure. In this study, the propulsive performance of three different rectangular panels with an aspect ratio of 2 are considered—rigid, chordwise flexible, and spanwise flexible. Free-swimming experiments are performed in a flow tank, from which the self-propelled speed and torque are measured in real time. From this, power and economy can be calculated as a function frequency and amplitude inputs. High-speed videography is taken during swimming and used to reconstruct the kinematics of the panel. With the rigid foil defining a baseline performance, the influence of chordwise and spanwise flexibility are examined and quantified. The results highlight the significant role that chordwise flexibility has on propulsive performance, specifically as it pertains to the economy. Spanwise flexibility does not appear to enhance the performance.

Nomenclature

A	=	amplitude of oscillation
f	=	frequency of oscillation
T	=	frequency of oscillation
R	=	radius of circle
κ	=	curvature of arc
c	=	chord
s	=	span
t	=	thickness
AR	=	aspect ratio
CoT	=	cost of transportation (economy)
U	=	speed
τ	=	servo torque
ω	=	servo angular speed
P	=	servo power
St	=	Strouhal number

[1] Ph.D. Student, rz6eg@virginia.edu, AIAA Student Member (Corresponding Author)
[2] Ph.D. Student, jw9un@virginia.edu, AIAA Student Member
[3] M.S. Student, gtl6eh@virginia.edu
[4] Research Scientist, jz8n@virginia.edu
[5] Associate Professor, haibo.dong@virginia.edu, AIAA Associate Fellow
[6] Professor, hb8h@virginia.edu
[7] Ph.D. Student, dylan.wainwright@gmail.com
[8] Professor, glauder@oeb.harvard.edu

I. Introduction

The main function of the caudal fin of thunniform swimming fish is for propulsion[1]. The high aspect ratio, lunate-shaped flexible tails of scombrid fishes such as mackerel and tuna contributed to high-speed, economical swimming and high thrust generation with low drag cost. Simplified physical models and more bio-inspired models have been developed to study the effects of shape and flexibility on swimming performance[2–8]. It is a challenge to uncouple these two parameters in order to quantify their respective roles in the propulsive performance. Attempts have been made to decompose underwater animal locomotion orthogonally[9,10]. For more simplified models, experimental flow tunnel tests of homogenous flexible foils[11–15] exhibit a combination of chordwise and spanwise deformations but the relative contributions cannot be determined. Additionally, the amount of flexion exhibited in either orientation is greatly influenced by the method of attachment at the leading edge. In almost all the flow tunnel tests, the homogeneous flexible foils exhibit dominantly chordwise flexibility, due to the common leading edge fixture method, where the leading edge is fully mounted to the pitching/heaving rod. The previous numerical study has explored the effects of spanwise versus chordwise flexibility of airfoil panels under low versus high Reynolds number condition[16]. The simulation prescribed pitching motion with pure chordwise or spanwise flexibility by changing the fixed boundary from leading edge to mid-span, which is challenging for real physical propulsor.

To address the challenges of these previous studies, two structurally anisotropic flexible panels have been designed and tested. One panel achieves chordwise flexibility, and one achieves spanwise flexibility. We focused on the steady swimming performance of the two panels and one rigid panel (as baseline case), by measuring their self-propelled speed, power consumption and kinematics over a frequency sweep inside a water tunnel. Using high-resolution videography, the experimental kinematics were reconstructed and used in immersed boundary method simulations[17,18] to investigate the flow structure.

We hypothesize that our anisotropic structure design can produce passive directional flexibility, without changing kinematic boundary conditions as in the previous numerical study. Also, the resulting change in propulsive performance will follow similar trends as in other studies of chordwise and spanwise flexibility in the water.

II. Materials and methods

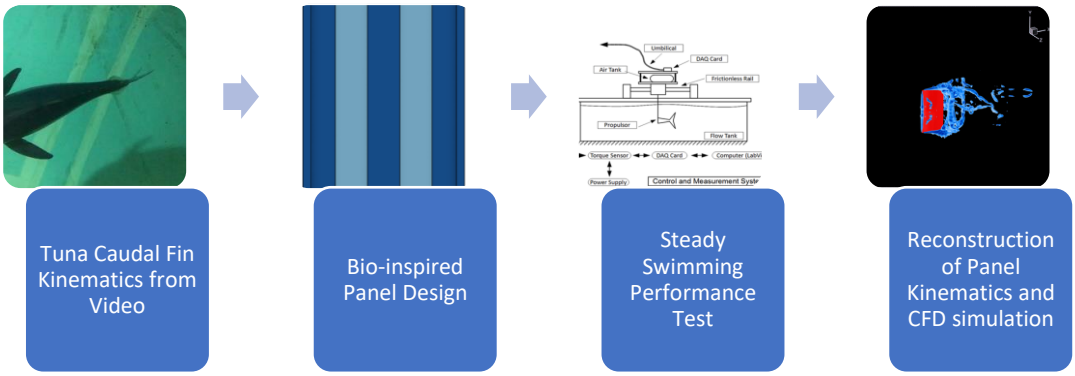

Figure 1. Workflow

A. Orthogonal decomposition of tuna caudal fin kinematics

Body and tail kinematics from freely-swimming yellowfin tuna (Thunnus albacares) were obtained at the Greenfins tuna facility at the University of Rhode Island courtesy of Prof. Terry Bradley, which is the first step of our workflow as shown in Fig. 1. Tuna swam in a 151,000-liter tank. Two synchronized Photron high-speed cameras were used to obtain high resolution (1 megapixel) dorsal and side views of the tail at 500 frames per second. As tuna moved past the side view camera and turned, we were able to obtain posterior views showing tail curvature from behind. Additional movies at 240 fps were obtained of tuna locomotion using iPhone 7 and GoPro Hero 4 cameras.

To study the directional flexibility in both directions, we define the Cartesian coordinate system as shown in Fig. 2: the fish is swimming forward in the negative x-direction; the gravity is in the negative y-direction; the z direction is pointing towards the left side of the fish. Under such coordinate system, the chordwise bending of the caudal fin is around the y-axis, while the spanwise bending is around the x-axis.

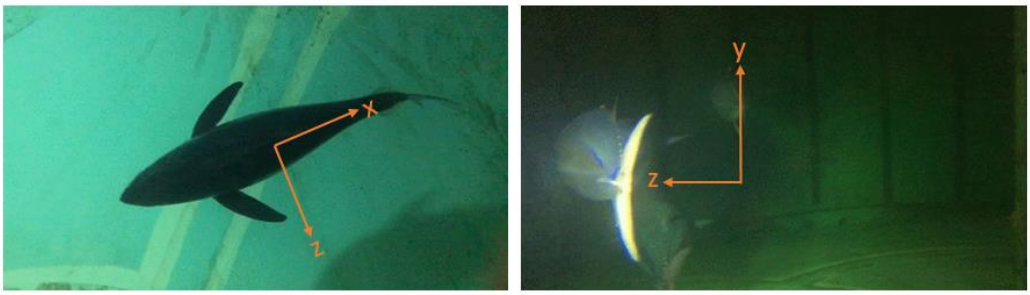

Figure 2. Coordinate system definition

We used Autodesk MAYA (Autodesk Inc., San Rafael, CA, USA) software to trace the 2D moving trajectory of tuna. Due to the circular shape of the tank, the tuna is maneuvering slightly. From the snapshots at 1/6 second segment as shown in Fig. 3, we can easily observe fin bending in the chordwise direction.

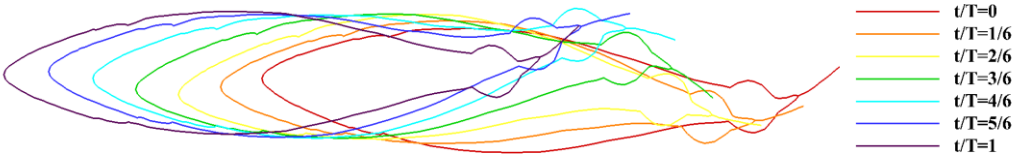

Figure 3. Trajectory of tuna in tank

B. Bio-inspired panel design

In this study, we focus primarily on the effects of flexibility, so the planform shape of the panel is fixed as a rectangular shape with span of 200 mm and chord of 100 mm. We choose this aspect ratio based on the previous measurement of scombrid fish caudal fins[19]. As shown, Westneat calculated the aspect ratio of caudal fin using the ratio of span squared to total fin area. Since we are using a rectangular panel as a simplified model, a rectangle passing the two fin tips and the front end of caudal fin for each of the original measurement is used as shown in Fig. 4. The aspect ratio of rectangle covering the caudal fin is then simply the ratio of span (height of the rectangle) to chord (width of the rectangle). As shown in Fig. 5, the average aspect ratio is 1.85 with a range of 1.22 to 2.48. We decide to choose $AR = 2$ for this specific study for ease of scaling the design of the structure.

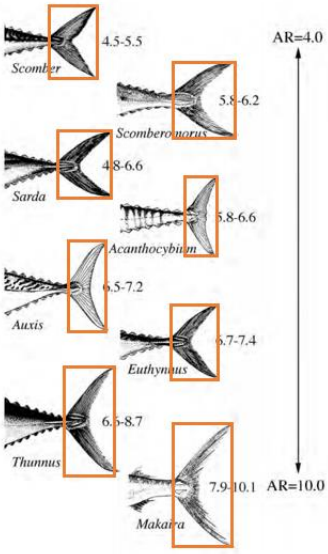

Figure 4. Caudal fin measurement
Adapted from Westneat & Wainwright 2001

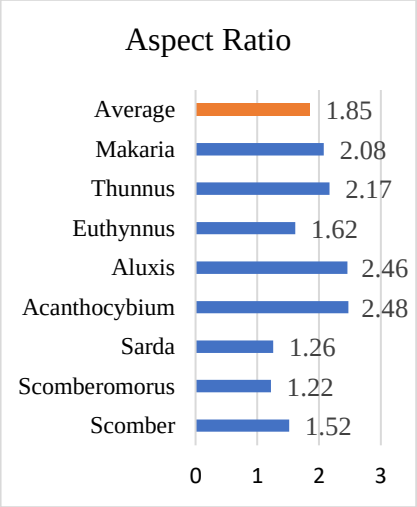

Figure 5. Caudal fin aspect ratio

When it comes to anisotropic flexibility, marine animals have many types of solution. For ray-fined fish, their fins are usually skeleton-enhanced flexible panels[20] that have different flexibility in parallel versus perpendicular direction of the fin rays. As shown in Fig. 6, a tuna caudal fin is composed of fin rays and more compliant membrane. The flexural modulus of fin rays has been determined by three-point bending tests to be within the range of 1 to 2 GPa. Inspired by the biostructure, we designed two panels with pure chordwise or spanwise flexibility.

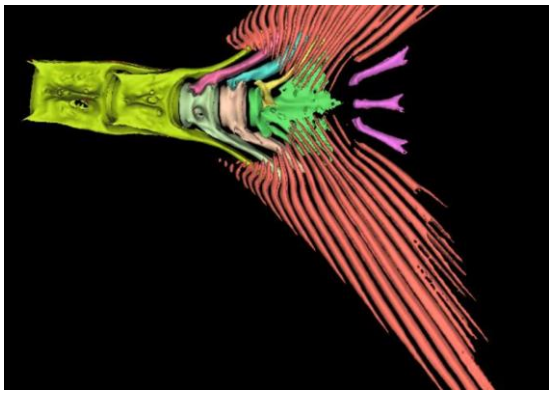

Figure 6. Tuna caudal fin CT scan

Figure 7 and 8 show the design of these two panels. In both cases, the main structure of panel is divided into five equally spaced sections in the flexible direction; two lightly colored sections have 1/6 thickness of the dark-colored sections, which theoretically should result in 216 times more deflection under the same load condition. The structure with dimensions listed in Table 1 is then printed using ABS plastic material with a flexural modulus of 1.65 to 2.1 GPa.

To allow flexibility in both direction, we employ a modified method to attach the panel to the driving rod. As shown in Fig. 7, 8 and 9, we use an additional fixture part to fix the mid 20 percent of mid-span and leading edge, so that the rest of the panel is free to bend under load.

Table 1. Dimensions of structure design

Property	Measurement (mm)
Chord *c*	100
Span *s*	200
Segment in Chord Direction	20
Segment in Span Direction	40
Thickness *t* (Darker)	1.5
Thickness *t* (Lighter)	0.25

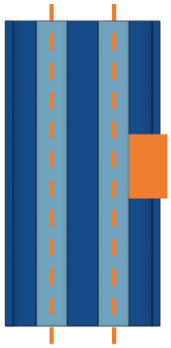

Figure 7. Chordwise flexible design

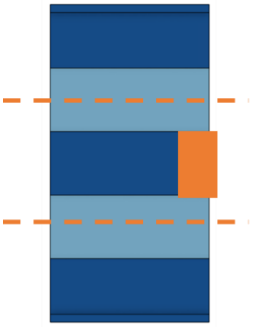

Figure 9. Spanwise flexible design

Figure 8. Panel fixture attached to rod

C. Water tunnel experimental setup

As depicted in Fig. 10, the system is a "water treadmill" based on a flow tunnel with changeable flow speed. The peduncle fixture is driven by a rod with a radius of 0.25 inch attached to a smart servo motor which operates in the optimal range of 0 to 3 Hz. When servo motor rotates, the panel generates a fish-tail-like oscillation which produces thrust. If the thrust equals the drag produced by the incoming flow, the panel stays swimming steadily, which is indicated by the laser distance reading on the user interface. Otherwise, the oscillating panel either moves forward or backward on the frictionless rail sustained by air-bearings.

The servo motor is connected to custom LabVIEW programs (National Instruments Crop., Austin, TX, USA), so that we can control the frequency and amplitude of pitching motion. The servo motor has a built-in torque sensor also connected through LabVIEW, so that we can measure the power consumption of servo motor by integrating the product of torque and arm over time.

A sequence of tests are run using the input parameters shown in Table 2, and servo torque and angular speed, and self-propelling speed of panels are recorded.

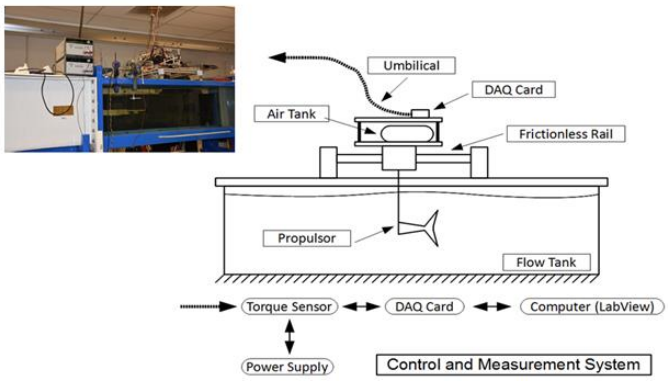

Figure 10. Flow tunnel setup

Table 2. Input and Output of Tests

	Rigid	Chordwise		Spanwise	
Input: Frequency *f* (0.25 Hz increment)	0.5 to 2.5 Hz	0.5 to 2.0 Hz		1 to 2.25 Hz	
Input: Amplitude *A*	30 deg on each side				
Output: Servo torque τ					
Output: Servo angular speed ω					
Output: Self-propelling speed *U*					

D. Kinematic reconstruction and CFD simulation

The panel kinematics inside the water tunnel is recorded as 60 fps videos, then imported into Autodesk MAYA software for reconstruction. Since each panel only demonstrates flexibility in one or fewer directions, we can reconstruct the motion using a 2d image sequence. As shown in Fig. 12, adding chordwise flexibility causes slight bending, which reduces trailing edge tip-to-tip amplitude compared to the rigid case in Fig. 11. Similarly, in Fig. 13, spanwise flexibility results in bending of the top and bottom edges of the panel, while the mid-span stays the same.

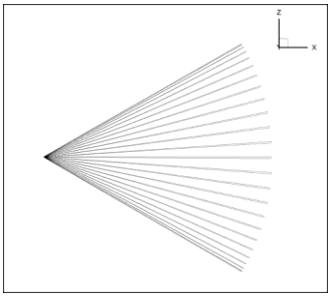

Figure 13. Rigid kinematics (top view)

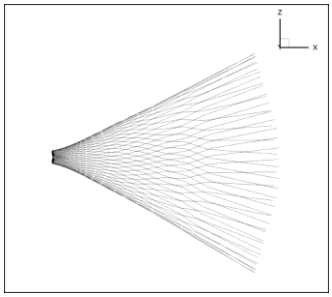

Figure 12. Chordwise flexible kinematics (top view)

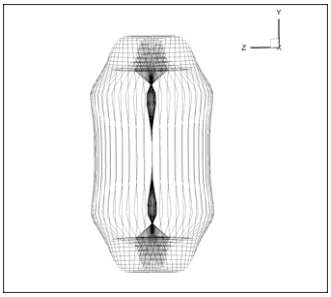

Figure 11. Spanwise flexible kinematics (back view)

III. Results

A. Passive fin bending observed from videos

There are many ways to define the amount of fin bending. Here we use the curvature method, which requires tracking of 3 points, as shown in Fig. 14 and Fig. 15. We break the video into images sequences using Adobe Photoshop and import images into MATLAB for tracking purpose. For the top view, we choose the start, middle and end point of the caudal fin, while for back view, we choose the top, center and bottom

point of the caudal fin. As long as the 3 points are not in one straight line, center location and radius of one and only circle can be determined. We also assign positive(negative) sign to the curvature value if the circle is on the left(right) side of the fish body.

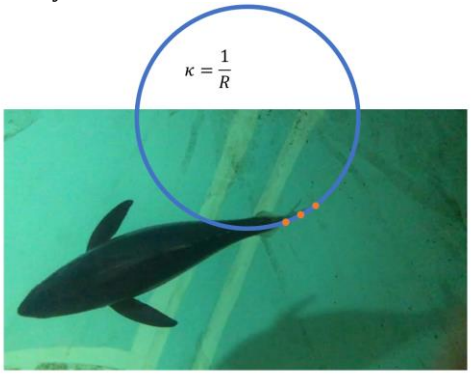

Figure 14. Chordwise curvature calculation

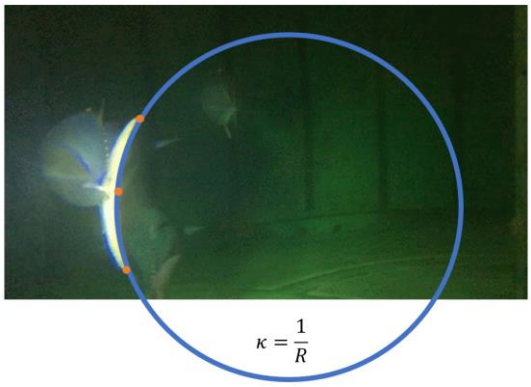

Figure 15. Spanwise curvature calculation

If we plot tail motion and curvature data over the same time axis, we find out there is a time lag between flapping motion and curvature, close to half cycle in both chordwise and spanwise views as shown in Fig. 16 & 17. This lag means when the tuna moves its caudal fin from left to right, the fin bends passively towards left, and vice versa.

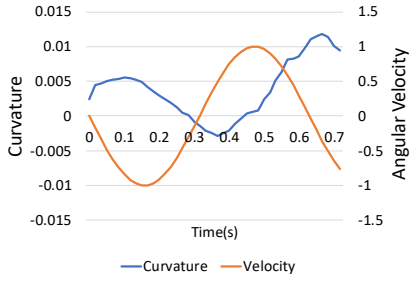

Figure 16. Chordwise curvature and angular velocity

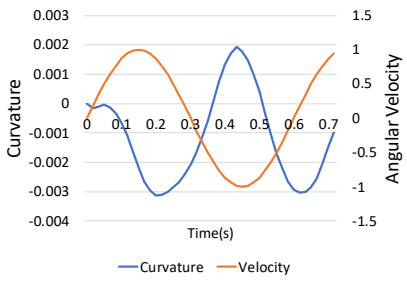

Figure 17. Spanwise curvature and angular velocity

Now if we compare the extent of bending by combining the two curvature plots as shown in Fig. 18, we find out that the caudal fin bends more in chordwise than spanwise direction.

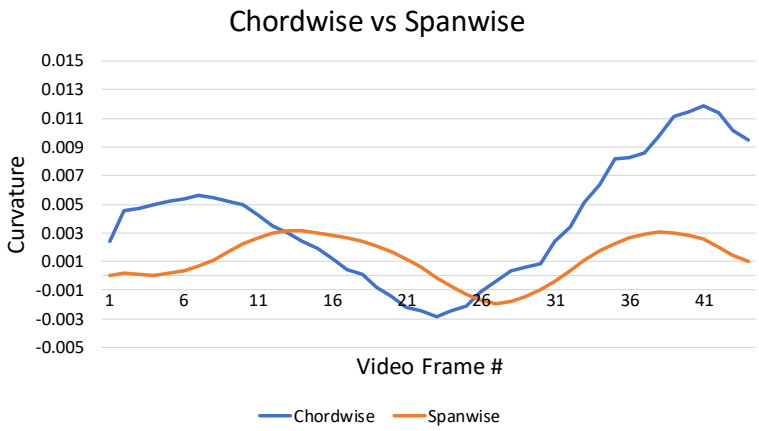

Figure 18. Chordwise versus spanwise curvature

B. Structural performance of panels

To validate that the bio-inspired structure does provide directional flexibility, we run finite element analysis (FEA) simulation on both flexible designs using Autodesk Inventor. The material properties are set as standard ABS plastics in Autodesk Material Library. Two point loads are exerted on the center of the top and bottom edge, while the mid-fifth of leading edge is fixed with cantilever beam condition.

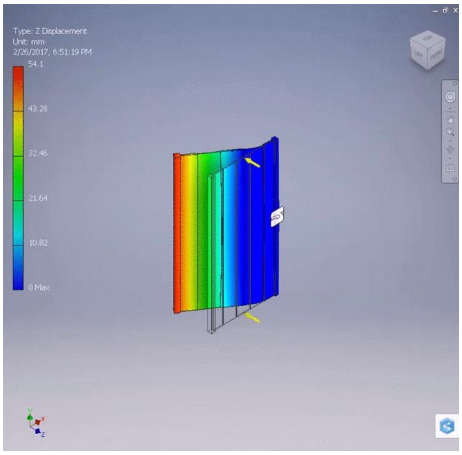

Figure 19. FEA simulation of chordwise flexbile panel

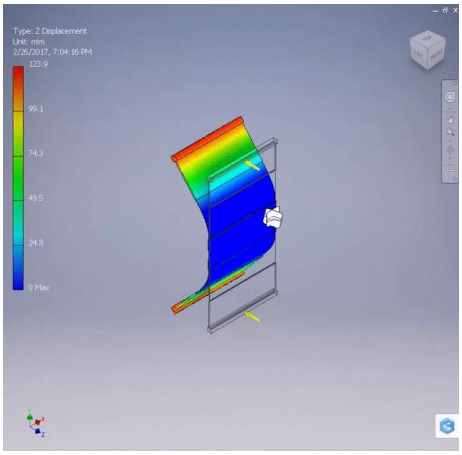

Figure 20. FEA simulation of spanwise flexbile panel

From the FEA results, we find out that the two panels show obvious directional flexibility as shown in Fig. 19 & 20, under the same boundary and load conditions. The properties in quasi-static test also exist in dynamic loading condition during the water tunnel test. We measured the tip-to-tip amplitude over the frequency range, and discovered there is a decreasing trend in tip amplitude for the chordwise flexible panel as shown in Fig. 21, while both the rigid and spanwise flexible panels show no decrease in tip amplitude.

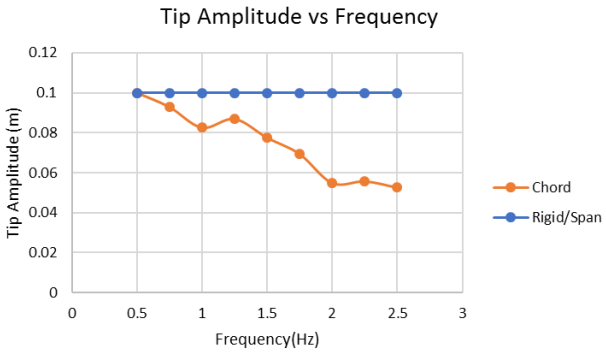

Figure 21. Tip amplitude vs. frequency

C. Propulsive performance: speed and efficiency

As mentioned earlier, the main input parameters to the tests are amplitude and frequency. Experiments using the three panels were performed with the frequency varied from 0.5 up to 2.5 Hz for the same input amplitude. The self-propelling speed was recorded and the results are shown in Fig. 22a. Compared to the rigid panel, there are clear disadvantages to having spanwise flexibility. The swimming speed attained at all frequencies is lower than that of the rigid foil. Chordwise flexibility does not improve swimming speed performance.

During the self-propelling tests, we measure the average power consumption by:

$$P = \overline{\tau\omega} \tag{1}$$

Then economy is calculated by:

$$CoT = \frac{P}{U} \tag{2}$$

When one now looks at the economy, it is clear that flexibility becomes important to performance. Fig 22b presents economy data for the three foils. It is clear that chordwise flexibility significantly increases economy of swimming—in some cases as much as 300%. Conversely, spanwise flexibility appears to be slightly detrimental to the swimming economy, coming very close to the economy of the rigid foil. By examining the Strouhal number, the chordwise flexible foil allows the artificial propulsor to operate in a range that produces efficient propulsion. As shown in Fig 22c, the rigid case shows increasing Strouhal number as frequency increases, while adding chordwise flexibility can keep the Strouhal number within the efficient region ($0.2 < St < 0.4$). Strouhal number is defined as:

$$St = \frac{fA}{U} \tag{3}$$

Last, the overall trend of economy versus Strouhal number, as shown in Fig. 22d is very similar compared to others' findings.

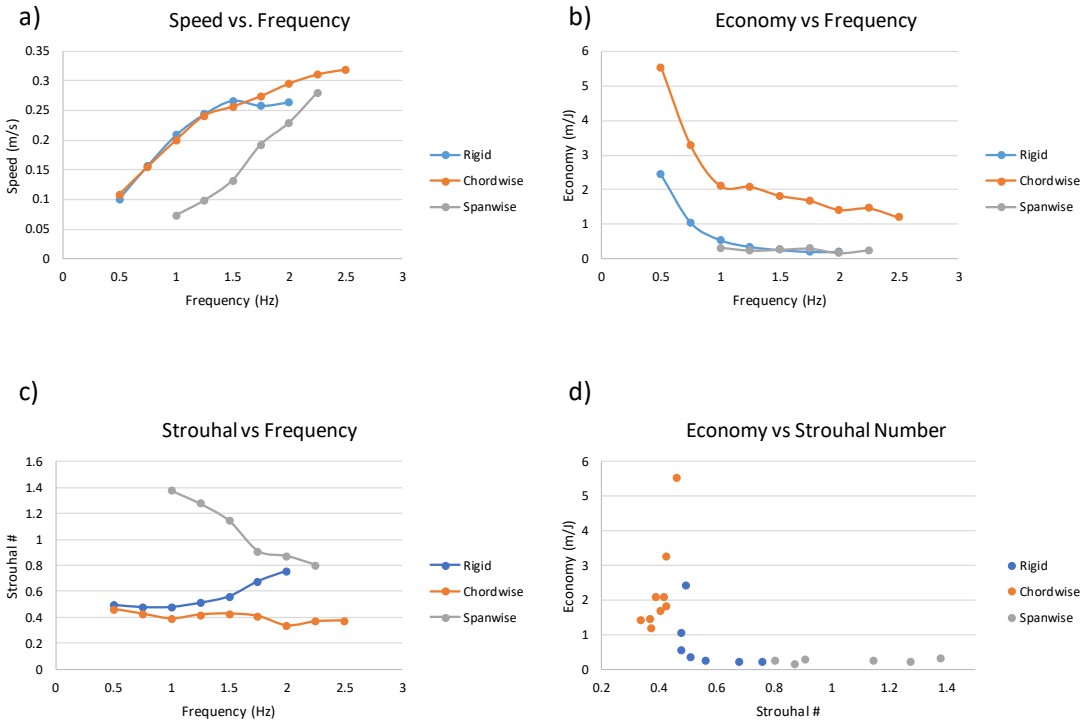

Figure 22. Flow tunnel test results

D. Flow structure

Using reconstructions of the kinematics from the tests, preliminary computational simulations to calculate the vortex flow structures were carried out. Using the immersed boundary method[17,18], we can determine the magnitude and time history of the hydrodynamic forces generated by the pitching panels. These preliminary results highlight some interesting features in the flow field that may explain the differences in performance measured experimentally. Take one frame as shown in Fig. 23 for example, adding chordwise flexibility reduces the amount of smaller-scale vortices, which have much less contribution to generating thrust compared to the large horseshoe vortex rings shed from the oscillating trailing edge.

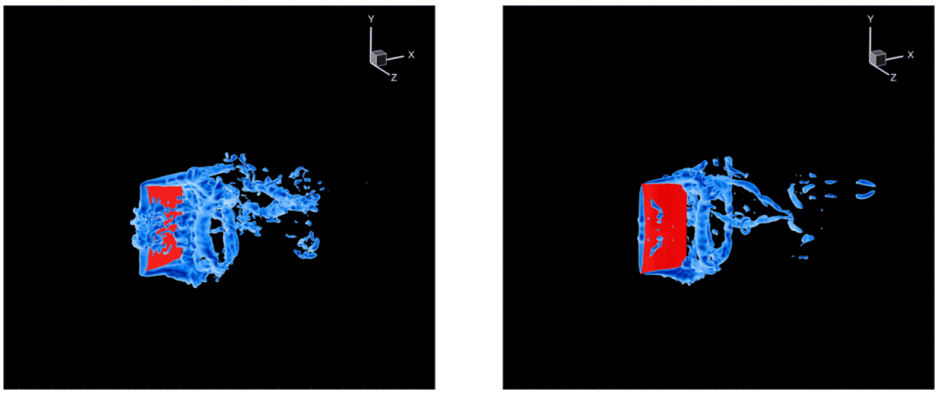

Rigid, $A = 30°$, $f = 2\ Hz$, begin of 4th cycle Chordwise, $A = 30°$, $f = 2\ Hz$, begin of 4th cycle

Figure 23. Flow structure of rigid vs. chordwise case

We look at the spanwise vortices surrounding the panel at the equivalent time frames for both rigid and chordwise flexible case, as shown in Fig. 24. We observe that the vortices are more concentrated and closer to the panel when we add the chordwise flexibility.

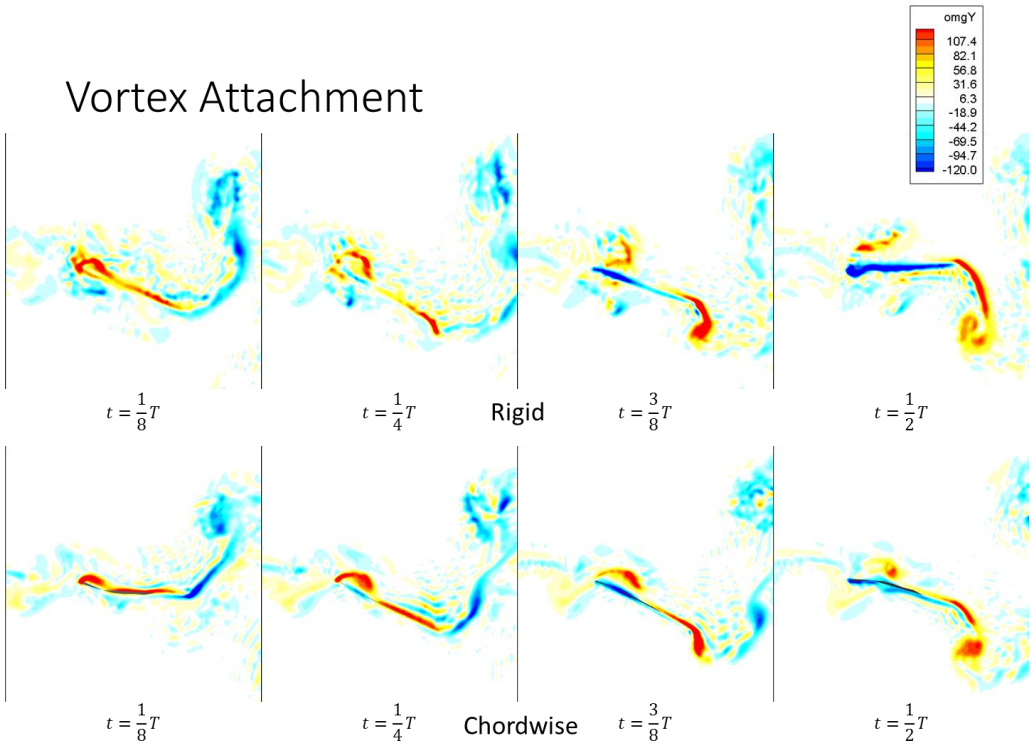

Figure 24. Vortex attachment of rigid vs. chordwise case

IV. Discussion

A. Effects of anisotropic flexibility on kinematics

Using the anisotropic panel design, we can achieve pure chordwise or spanwise flexibility without changing the boundary fixture condition. Given the current structure design and material properties, chordwise flexibility keeps the spans including trailing edge vertically straight, while reducing the horizontal tip amplitude as frequency increases. On the other hand, spanwise flexibility keeps the chords including top and bottom edge horizontally straight, while reducing the tip amplitude near the top and bottom edges. However, if we only look at the midspan of the spanwise flexible case, the amplitude stays same for Strouhal number calculation.

B. Effects of anisotropic flexibility on propulsive performance

Our results agree with previous numerical work[16], that chordwise flexibility increases the efficiency of pitching panels, while spanwise flexibility decreases both thrust and efficiency. Our conclusion is backed not only by water tunnel measurement, but also by preliminary CFD flow visualization showing that chordwise flexibility results in cleaner flow structure and better vortex attachment.

C. Comparison to live tuna

As we observed in real tuna kinematics, there is a greater degree of chordwise bending compared to spanwise, which suggest that overall the anisotropic flexibility should enhance the propulsive efficiency of tuna caudal fin. We are still making a lot of assumptions at the early state: we use a rectangular panel instead of a shape closer to biology; we isolate the directional flexibility instead of combining; the fin-ray inspired

structure is coarser than biology; the leading edge motion is pure pitching. In future work, we plan to make modification in these aspects, and study the effects of anisotropic flexibility in a more bio-mimetic setup.

V. Conclusion

Using simplified models, we succeed in isolating directional flexibility and study their effects on swimming performance. Results show that chordwise flexibility improved the swimming performance of a free-swimming panel compared to a rigid one. For future studies, more bio-fidelity models with 3D complex geometry and deformation must be studied, in order to fully understand the biomechanics and fluid dynamics behind fish swimming.

Acknowledgments

This work was supported by ONR MURI grant N00014-14-1-0533 (monitored by Dr Robert Brizzolara) and the David and Lucille Packard Foundation.

References

[1] Lauder, G. V., Flammang, B., and Alben, S., "Passive robotic models of propulsion by the bodies and caudal fins of fish," *Integrative and Comparative Biology*, vol. 52, 2012, pp. 576–587.

[2] Affleck, R. J., "Some points in the function, development and evolution of the tail in fishes," *Proceedings of the Zoological Society of London*, vol. 120, 1950, pp. 349–368.

[3] Lighthill, M. J., "Aquatic animal propulsion of high hydromechanical efficiency," *Journal of Fluid Mechanics*, vol. 44, Nov. 1970, p. 265.

[4] Wu, T. Y.-T., "Hydromechanics of swimming propulsion. Part 2. Some optimum shape problems," *Journal of Fluid Mechanics*, vol. 46, Apr. 1971, p. 521.

[5] Chopra, M. G., "Hydromechanics of lunate-tail swimming propulsion," *Journal of Fluid Mechanics*, vol. 64, Jan. 1974, pp. 375–391.

[6] Karpouzian, G., Spedding, G., and Cheng, H. K., "Lunate-tail swimming propulsion. Part 2. Performance analysis," *Journal of Fluid Mechanics*, vol. 210, 1990, p. 329.

[7] Borazjani, I., and Daghooghi, M., "The fish tail motion forms an attached leading edge vortex.," *Proceedings. Biological sciences / The Royal Society*, vol. 280, 2013, p. 20122071.

[8] Feilich, K. L., and Lauder, G. V, "Passive mechanical models of fish caudal fins: effects of shape and stiffness on self-propulsion," *Bioinspiration & Biomimetics*, vol. 10, 2015, p. 36002.

[9] Fish, F., Schreiber, C., Moored, K., Liu, G., Dong, H., and Bart-Smith, H., "Hydrodynamic Performance of Aquatic Flapping: Efficiency of Underwater Flight in the Manta," *Aerospace*, vol. 3, Jul. 2016, p. 20.

[10] Liu, G., Ren, Y., Zhu, J., Bart-Smith, H., and Dong, H., "Thrust producing mechanisms in ray-inspired underwater vehicle propulsion," *Theoretical and Applied Mechanics Letters*, vol. 5, 2015, pp. 54–57.

[11] Dewey, P. a., Boschitsch, B. M., Moored, K. W., Stone, H. a., and Smits, a. J., "Scaling laws for the thrust production of flexible pitching panels," *Journal of Fluid Mechanics*, vol. 732, 2013, pp. 29–46.

[12] Kancharala, a K., and Philen, M. K., "Study of flexible fin and compliant joint stiffness on propulsive performance: theory and experiments.," *Bioinspiration & biomimetics*, vol. 9, 2014, p. 36011.

[13] Shelton, R. M., Thornycroft, P. J. M., and Lauder, G. V, "Undulatory locomotion of flexible foils as biomimetic models for understanding fish propulsion.," *The Journal of experimental biology*, vol. 217, 2014, pp. 2110–20.

[14] Quinn, D. B., Lauder, G. V, and Smits, A. J., "Scaling the propulsive performance of heaving flexible panels," *Journal of Fluid Mechanics*, vol. 738, 2014, pp. 250–267.

[15] Quinn, D. B., Lauder, G. V., and Smits, A. J., "Maximizing the efficiency of a flexible propulsor using experimental optimization," *Journal of Fluid Mechanics*, vol. 767, 2015, pp. 430–448.

[16] Zhu, Q., "Numerical Simulation of a Flapping Foil with Chordwise or Spanwise Flexibility," *AIAA Journal*, vol. 45, 2007, pp. 2448–2457.

[17] Mittal, R., Dong, H., Bozkurttas, M., Najjar, F. M., Vargas, A., and von Loebbecke, A., "A versatile sharp interface immersed boundary method for incompressible flows with complex boundaries," *Journal of Computational Physics*, vol. 227, 2008, pp. 4825–4852.

[18] Wan, H., Dong, H., and Gai, K., "Computational investigation of cicada aerodynamics in forward

flight."
[19] Westneat, M. W., and Wainwright, S. A., "7. Mechanical design for swimming: muscle, tendon, and bone," *Fish Physiology*, vol. 19, 2001, pp. 271–311.
[20] Lauder, G. V., Madden, P. G. a, Tangorra, J. L., Anderson, E., and Baker, T. V, "Bioinspiration from fish for smart material design and function," *Smart Materials and Structures*, vol. 20, 2011, p. 94014.